NASA TECHNICAL NOTE

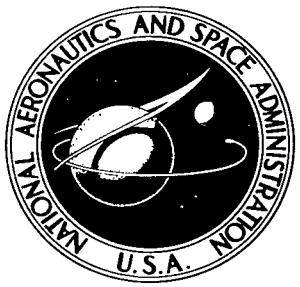

NASA TN D-2035

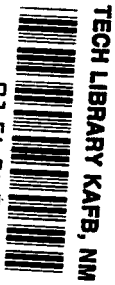

NASA TN D-2035

LANDING CHARACTERISTICS OF A REENTRY VEHICLE WITH A PASSIVE LANDING SYSTEM FOR IMPACT ALLEVIATION

by Sandy M. Stubbs

Langley Research Center
Langley Station, Hampton, Va.

NATIONAL AERONAUTICS AND SPACE ADMINISTRATION • WASHINGTON, D. C. • JANUARY 1964

LANDING CHARACTERISTICS OF A REENTRY VEHICLE WITH A PASSIVE LANDING SYSTEM FOR IMPACT ALLEVIATION

By Sandy M. Stubbs

Langley Research Center
Langley Station, Hampton, Va.

Technical Film Supplement L-807 available on request.

NATIONAL AERONAUTICS AND SPACE ADMINISTRATION

For sale by the Office of Technical Services, Department of Commerce,
Washington, D.C. 20230 -- Price $0.75

LANDING CHARACTERISTICS OF A REENTRY VEHICLE WITH A PASSIVE LANDING SYSTEM FOR IMPACT ALLEVIATION

By Sandy M. Stubbs

SUMMARY

An experimental investigation was made to determine the landing characteristics of a 1/8-scale dynamic model of a reentry vehicle using a passive landing system to alleviate the landing-impact loads. The passive landing system consisted of a flexible heat shield with a small section of aluminum honeycomb placed between the heat shield and the crew compartment at the point that would be the first to contact the landing surface. The model was landed on concrete and sand landing surfaces at parachute letdown velocities. The investigations simulated a vertical velocity of 30 ft/sec (full scale), horizontal velocities of 0, 15, 30, 40, and 50 ft/sec (full scale), and landing attitudes ranging from -30° to 20°.

The model investigation indicated that stable landings could be made on a concrete surface at horizontal velocities up to about 30 ft/sec, but the stable landing-attitude range at these speeds was small. The aluminum honeycomb bottomed occasionally during landings on concrete. When bottoming did not occur, maximum normal and longitudinal accelerations at the center of gravity of the vehicle were approximately 50g and 30g, respectively.

Results indicated stable landings could be made on sand for a wide range of horizontal velocities and negative landing attitudes. Maximum normal and longitudinal accelerations at the center of gravity of the vehicle were approximately 40g and 24g, respectively, for landings on sand. The aluminum honeycomb did not bottom during landings on sand.

INTRODUCTION

Manned spacecraft, when landed by parachute, generally require some method of alleviating the landing-impact loads. The evaluation and development of efficient spacecraft landing systems that are simple, reliable, and adaptable to various landing environments are of continuing interest. Since anticipated infrequent landings of spacecraft allow the use of a "one-shot" type landing system, the qualities of simplicity and reliability are especially desirable. A great deal of interest in passive landing systems for spacecraft exists because they possess these desirable qualities. A passive landing system is one in which deployment of the heat shield or other devices is not necessary. Previous investigations of passive landing systems at parachute letdown velocities have been limited to landings on water. (See, for example, refs. 1, 2, and 3.) Recovery

requirements indicate a need for the reentry vehicle to have a capability of landing on land as well as on water. The purpose of the present investigation was to determine the accelerations and landing characteristics of a reentry vehicle landing on land with a passive landing system.

In the present investigation it was assumed that sufficient control of the attitude of the vehicle was available to assure contact on a predetermined area of the vehicle heat shield. Attitude control permits the use of a lightweight impact alleviator placed in the area of impact. The passive landing system consisted of a flexible heat shield that would oilcan and a small section of aluminum honeycomb (impact alleviator) placed between the heat shield and the crew compartment. Because of the limited stroke of this type of passive landing system, additional shock attenuators might be necessary for the crew couches; however, couch attenuators were not tested in the present investigation.

A 1/8-scale dynamic model of a proposed three-man spacecraft was used in the investigation. The model was tested at a vertical velocity of 30 ft/sec (full scale) and horizontal velocities of 0, 15, 30, 40, and 50 ft/sec (full scale). Landings were made on concrete and sand landing surfaces at attitudes ranging from -30° to 20°. Results presented in reference 4 indicate that negative landing attitudes are more stable than positive attitudes; hence, most of the tests were made at negative landing attitudes. The tests were conducted in the Langley impact structures facility.

A short motion-picture film supplement illustrating the landing motions of the model has been prepared and is available on loan. A request card form and a description of the film will be found at the back of this paper on the page with the abstract cards.

DESCRIPTION OF MODEL

The model used in the investigation was a 1/8-scale dynamic model of a proposed three-man reentry vehicle. Figure 1 shows the general arrangement of the model. The model was constructed of fiber glass and plastic, with the lower section of the crew compartment made of solid balsa wood. Mahogany blocks were potted in the balsa wood to serve as accelerometer mounts. (See fig. 2.) The model weight (13.83 lb) simulated a full-scale weight of 7,080 pounds based on the scale relationships shown in table I. Pertinent dimensions and moment-of-inertia measurements are listed in table II. All values reported are full scale unless otherwise indicated. Photographs of the model are shown in figure 3.

The passive landing system consisted of a flexible heat shield and a small section of aluminum honeycomb located between the heat shield and the crew compartment. The flexible heat shield was constructed of fiber glass and plastic and was 0.020 inch thick. The heat shield was designed to oilcan under impact loads. The aluminum honeycomb used was made of 3003-H19 aluminum with a 1/4-inch cell size and 0.001-inch wall thickness. A section 2 inches in diameter was placed between the heat shield and the crew compartment. The honeycomb was placed at the point on the heat shield that would be the first to contact the

landing surface. This contact point varied with changes in landing attitude. (See fig. 2.) The honeycomb was precrushed to obtain a more desirable force time history. The precrushed shape matched the spherical radii of the heat shield and the crew compartment, and the honeycomb was securely attached at both surfaces to reduce shearing and rebound. For the test attitude range, the thickness of the honeycomb varied from 0.93 to 1.08 inches because of the offset center line of the crew compartment with respect to the center line of the heat shield.

APPARATUS AND PROCEDURE

Tests of the 1/8-scale model were made at parachute letdown velocities corresponding to a vertical velocity of 30 ft/sec and to horizontal velocities of 0, 15, 30, 40, and 50 ft/sec. Figure 4 shows the model acceleration axes, flight path, force directions, and landing attitudes. The model was landed on concrete and sand landing surfaces at landing attitudes from -30° to 20°. The coefficient of sliding friction between the concrete landing surface and the model was approximately 0.35. The sand-landing tests were conducted with loose dry Standard Ottawa Testing Sand. This sand was not meant to represent any particular terrain but was chosen because its controlled uniform characteristics favor reproducible experiments. The drag force was not determined for the sand landing surface because the drag force varies with sand penetration.

Six strain-gage accelerometers were used to measure accelerations. Normal, longitudinal, and angular accelerations were measured about the center of gravity of the vehicle, and normal and longitudinal accelerations were measured at the center of gravity of the crew couch. (See fig. 1.) The electronic characteristics of the accelerometers used in the investigation are presented in table III. The signals from the accelerometers were transmitted through trailing cables to the recording equipment. The response of the recording equipment (control box, oscillograph, and galvanometers) was flat to 135 cps.

Figure 5 is a sketch showing the launch procedure. The pendulum was released from a predetermined height to produce the desired horizontal velocity. At the end of one-quarter period, the model was released, and the free fall gave the desired vertical velocity. The model was attached to the launch carriage by an electromagnet, as shown in figure 6. The model release mechanism was a photocell designed to open the electromagnet electrical circuit and allow the model to fall free. Motion pictures were made to record the landing behavior of the model.

RESULTS AND DISCUSSION

Acceleration

Typical oscillograph records of accelerations are shown in figures 7 and 8. Figure 7 shows acceleration time histories and maximum accelerations for landings on concrete. Figure 7(a) is an oscillograph record of a vertical landing at an

attitude angle of -16°, and figure 7(b) is the record of a landing with a horizontal velocity at an attitude angle of -18°. Figure 8 shows time histories and maximum accelerations for landings on sand. Figure 8(a) shows the results for a vertical landing at an attitude angle of -16°, and figure 8(b) shows the results for a landing with a horizontal velocity at an attitude angle of -15°. The dashed lines are fairings of the accelerometer traces. Maximum acceleration data presented in figures 9 to 13 were obtained from similar fairings.

Normal acceleration.- Acceleration data are shown in figures 9 to 13. Figure 9 shows maximum normal accelerations at the center of gravity of the vehicle for landings on both concrete and sand landing surfaces. The shaded data points indicate that the model turned over, and the flagged data points indicate bottoming. Bottoming occurred when the passive landing system failed to dissipate all the energy due to vertical velocity of the vehicle, and, as a result, all of the available stroke of the honeycomb was used. When bottoming occurred the maximum accelerations were appreciably higher than in tests in which bottoming did not occur. The data points for which bottoming occurred are not considered in discussing the acceleration trends.

For the landings made on concrete (fig. 9(a)), there was an increase in normal acceleration from 16g at a landing attitude of -30° to approximately 50g at a landing attitude of about -5°. There was no discernible effect of horizontal velocity on normal accelerations. For landings made on sand (fig. 9(b)), there was an increase in normal accelerations from 12g at a landing attitude of -30° to approximately 40g at a landing attitude of -5°. Bottoming did not occur during the landings on sand, and horizontal velocity had no effect on normal accelerations.

Figure 10 shows maximum normal accelerations at the center of gravity of the crew couch. The same trends appear at the center of gravity of the crew couch that appeared at the center of gravity of the vehicle; however, the spread in maximum accelerations was slightly greater. For landings on concrete (fig. 10(a)), maximum normal accelerations at the center of gravity of the couch range from 12g at a landing attitude of -30° to 63g at a landing attitude of -5°. For landings on sand (fig. 10(b)), maximum normal accelerations at the center of gravity of the couch range from 10g at a landing attitude of -30° to 55g at a landing attitude of -5°.

Normal accelerations in the attitude range between -15° and 15° were greater than safe human tolerance levels indicated in reference 5. Thus, if landings at attitudes between -15° and 15° are to be attempted, it would seem necessary to have a separate crew-couch attenuation system with a stroke capability greater than that of the passive landing system reported herein.

Longitudinal acceleration.- Maximum longitudinal accelerations at the center of gravity of the vehicle and at the center of gravity of the crew couch are presented in figures 11 and 12, respectively. The maximum longitudinal accelerations for landings on concrete (fig. 11(a)) ranged from 18g at a landing attitude of -30° to about 30g at a landing attitude of -10°. There was no discernible effect of horizontal velocity on longitudinal accelerations for landings on concrete. The maximum longitudinal accelerations for landings on sand

(fig. 11(b)) ranged from approximately 10g to 24g over the test range of negative landing attitudes. Essentially no effect of landing attitude on longitudinal accelerations was noted for landings on sand; however, there does appear to be a slight increase in longitudinal acceleration with an increase in horizontal velocity for landings on sand. The longitudinal accelerations at the center of gravity of the crew couch (fig. 12) showed the same trends and were at the same acceleration levels as those at the center of gravity of the vehicle.

Angular acceleration.- The maximum angular accelerations of the vehicle for landings on concrete and sand are shown in figure 13. Several runs were omitted from figure 13 because the angular accelerations exceeded the range of the accelerometers. The maximum angular accelerations for landings on concrete, shown in figure 13(a), ranged from 60 to 200 radians per second per second in a pitch nose-up direction. The maximum angular accelerations for landings on sand, presented in figure 13(b), ranged from a nose-up pitching acceleration of 140 radians per second per second to a nose-down pitching acceleration of 120 radians per second per second for landing attitudes from -20° to 0°.

Stability

Figure 14 shows the stability of the model when landed on a concrete landing surface. The test conditions are shown as circle data points with the shaded circles indicating turnover. Horizontal velocity appears to have an effect on stability. This effect may be due to landing-surface roughness, friction changes, angular velocity of the model at impact, or other varying parameters. The data presented in figure 14 indicate that stable landings can be made on concrete for a limited attitude range at horizontal velocities up to about 30 ft/sec.

The stability of the model when landed on a sand landing surface is shown in figure 15. There is an effect of horizontal velocity on stability that is due in part to an increase in time through which the drag force is applied. The drag force also increased because of penetration of the sand when the vehicle was sliding at high negative landing attitudes. This penetration resulted in a "tripping" action which adversely affected the vehicle stability. The dashed line indicates the separation of the stable and unstable regions. The results presented in figure 15 indicate that stable landings could be made over a wide range of horizontal velocities and negative landing attitudes.

SUMMARY OF RESULTS

The landing tests of a 1/8-scale dynamic spacecraft model having a passive landing system consisting of a flexible heat shield backed up by a section of crushable honeycomb led to the following results:

1. The passive landing system had stable landing behavior in landings on concrete for horizontal velocities up to about 30 ft/sec, but the stable landing-attitude range at these speeds was limited.

2. Maximum normal and longitudinal accelerations at the center of gravity of the vehicle were approximately 50g and 30g, respectively, for landings on concrete, except when bottoming occurred and gave higher accelerations.

3. Stable landings could be made on loose sand for a wide range of horizontal velocities and negative landing attitudes.

4. Maximum normal and longitudinal accelerations at the center of gravity of the vehicle were approximately 40g and 24g, respectively, for landings on sand. The aluminum honeycomb did not bottom during landings on sand.

5. Additional shock attenuators for the crew couches would be necessary should the spacecraft be landed at attitudes between -15° and 15°.

Langley Research Center,
National Aeronautics and Space Administration,
Langley Station, Hampton, Va., August 27, 1963.

REFERENCES

1. McGehee, John R., Hathaway, Melvin E., and Vaughan, Victor L., Jr.: Water-Landing Characteristics of a Reentry Capsule. NASA MEMO 5-23-59L, 1959.

2. Vaughan, Victor L., Jr.: Water-Landing Impact Accelerations for Three Models of Reentry Capsules. NASA TN D-145, 1959.

3. Vaughan, Victor L., Jr.: Landing Characteristics and Flotation Properties of a Reentry Capsule. NASA TN D-653, 1961.

4. Stubbs, Sandy M.: Investigation of the Skid-Rocker Landing Characteristics of Spacecraft Models. NASA TN D-1624, 1963.

5. Eiband, A. Martin: Human Tolerance to Rapidly Applied Accelerations: A Summary of the Literature. NASA MEMO 5-19-59E, 1959.

TABLE I.- SCALE RELATIONSHIPS

[λ = Scale of model]

Quantity	Full-scale value	Scale factor	Model
Length	l	λ	λl
Area	A	λ^2	$\lambda^2 A$
Weight	W	λ^3	$\lambda^3 W$
Moment of inertia	I	λ^5	$\lambda^5 I$
Time	t	$\sqrt{\lambda}$	$\sqrt{\lambda} t$
Speed	v	$\sqrt{\lambda}$	$\sqrt{\lambda} v$
Linear acceleration	a	1	a
Angular acceleration	α	λ^{-1}	$\lambda^{-1}\alpha$
Force	F	λ^3	$\lambda^3 F$

TABLE II.- PERTINENT PARAMETERS OF REENTRY VEHICLE

	1/8-scale model	Full-scale vehicle
Gross weight, lb	13.83	7,080
Moment of inertia (approx.), slug-ft^2:		
I_X (roll)	0.058	1,900
I_Y (pitch)	0.078	2,550
I_Z (yaw)	0.095	3,100
Body:		
Diameter, in.	19.25	154.00
Height, in.	11.19	89.52

TABLE III.- ACCELEROMETER CHARACTERISTICS

Accelerometer orientation	Range, g units	Natural frequency, cps	Damping, percent of critical damping
At the center of gravity of the vehicle			
Normal	±100	700	60
Longitudinal	±50	627	65
Angular	±50	312	60
At the center of gravity of the couch			
Normal	±50	444	100
Longitudinal	±50	444	80

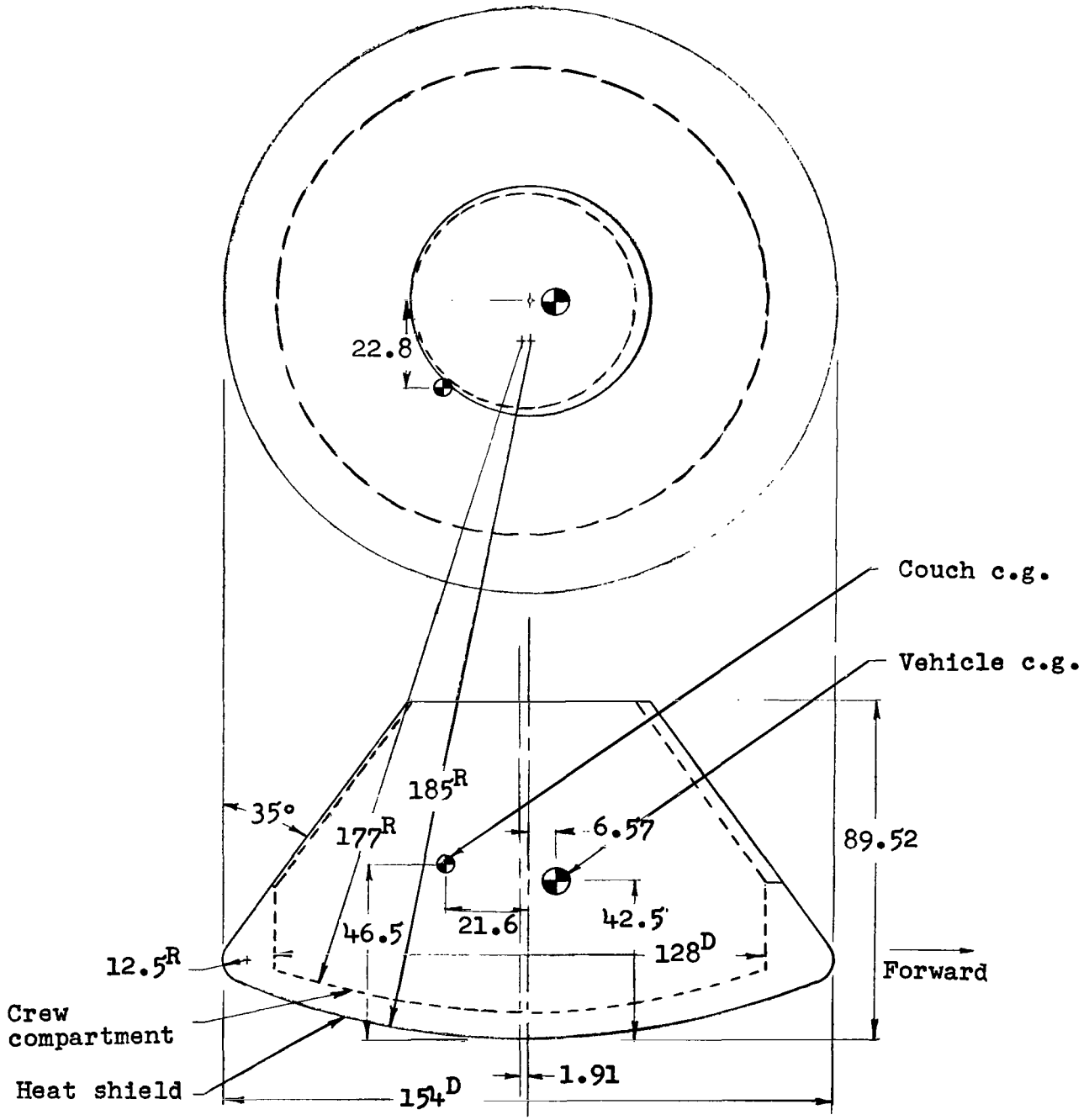

Figure 1.- General arrangement of 1/8-scale dynamic model of a three-man reentry vehicle. All dimensions are in inches, full scale.

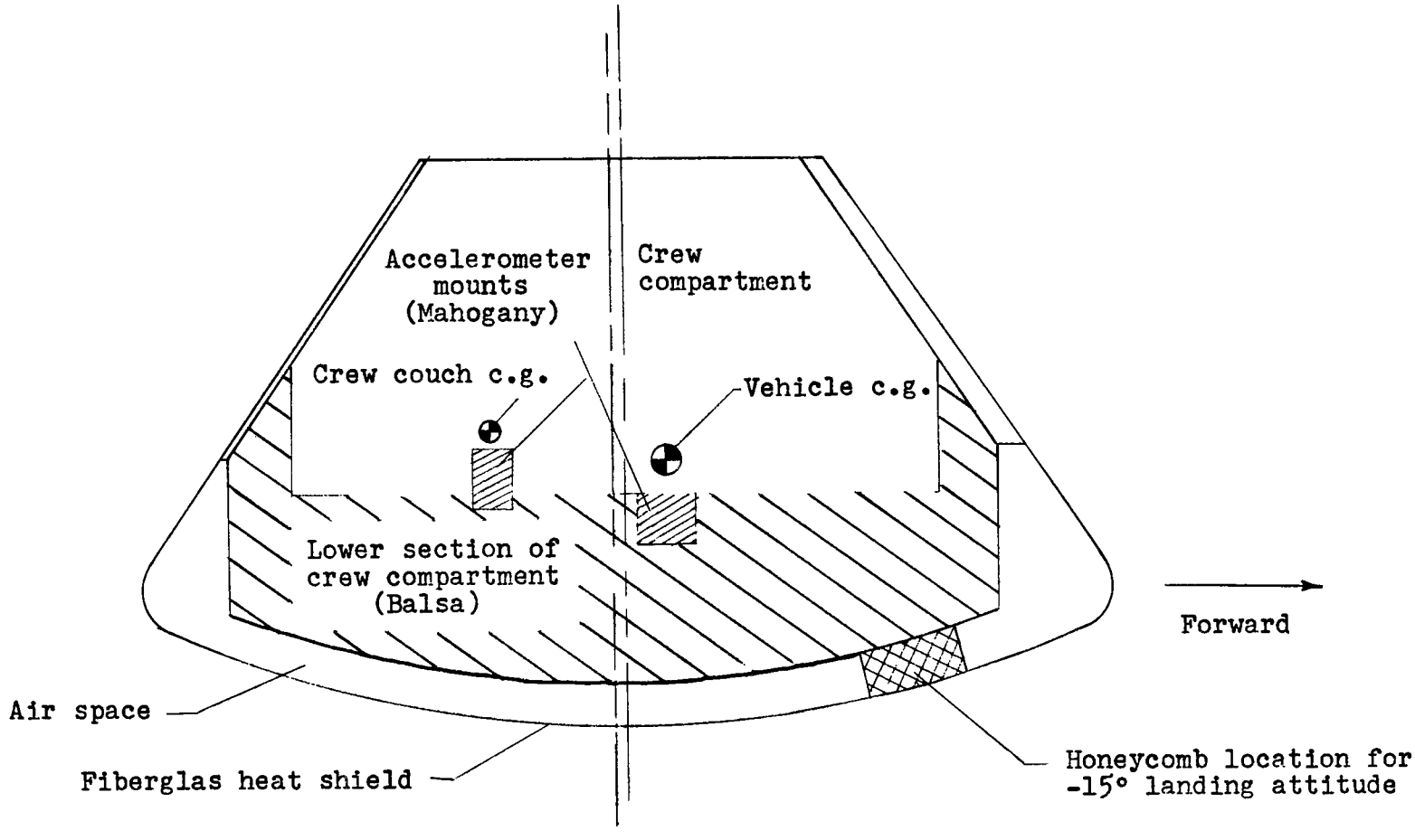

Figure 2.- Sketch of model construction and honeycomb location.

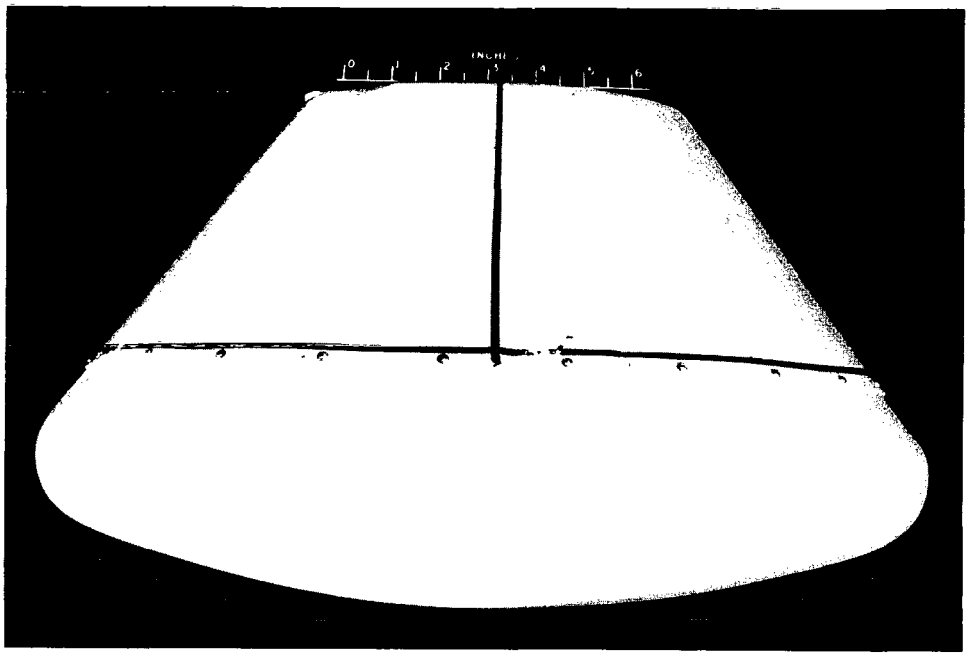

(a) Flexible heat shield attached. L-62-4446

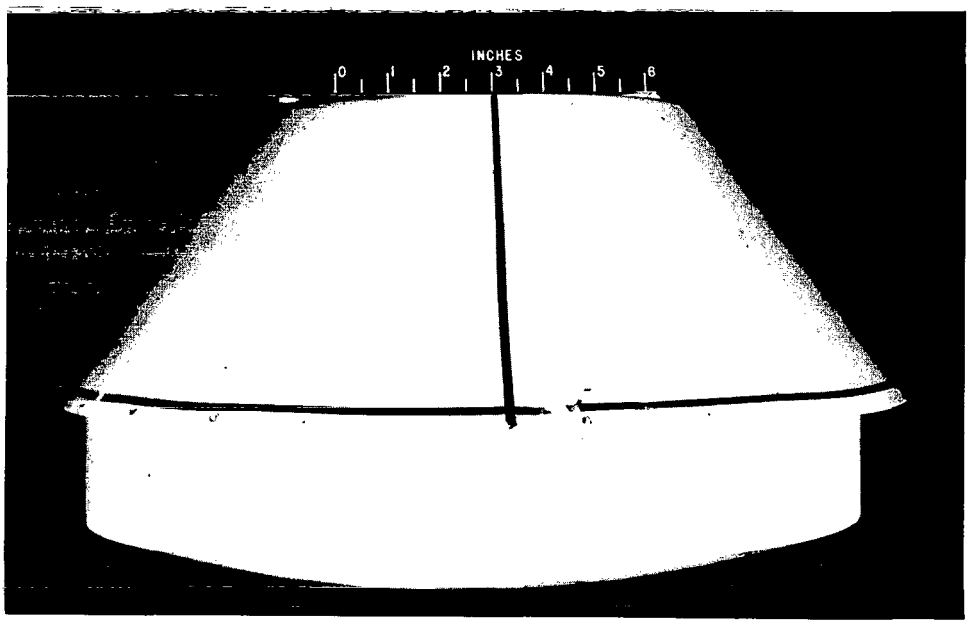

(b) Heat shield removed. L-62-4448

Figure 3.- Photographs of 1/8-scale model.

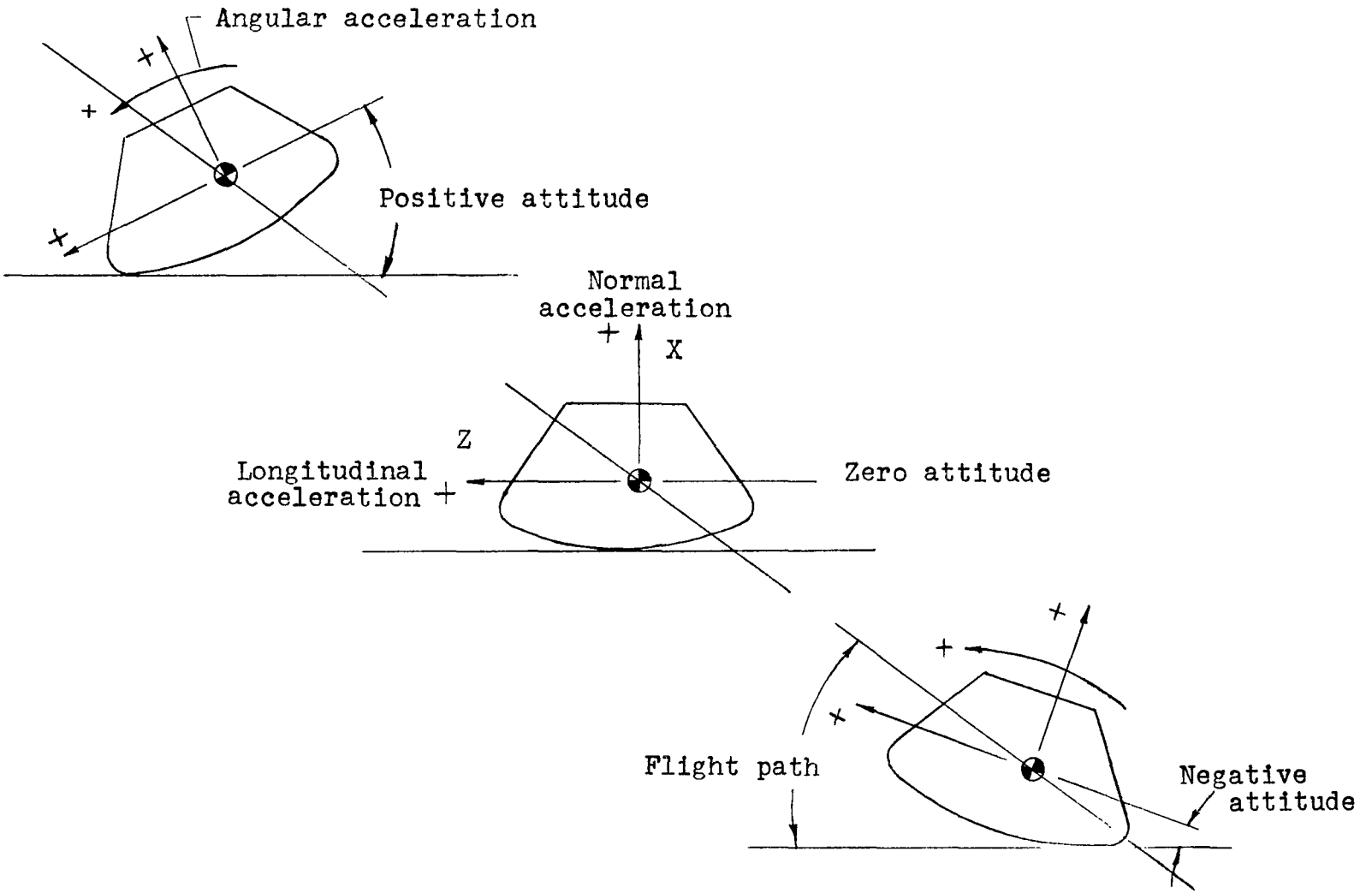

Figure 4.- Sketches identifying acceleration axes, attitudes, force directions, and flight path.

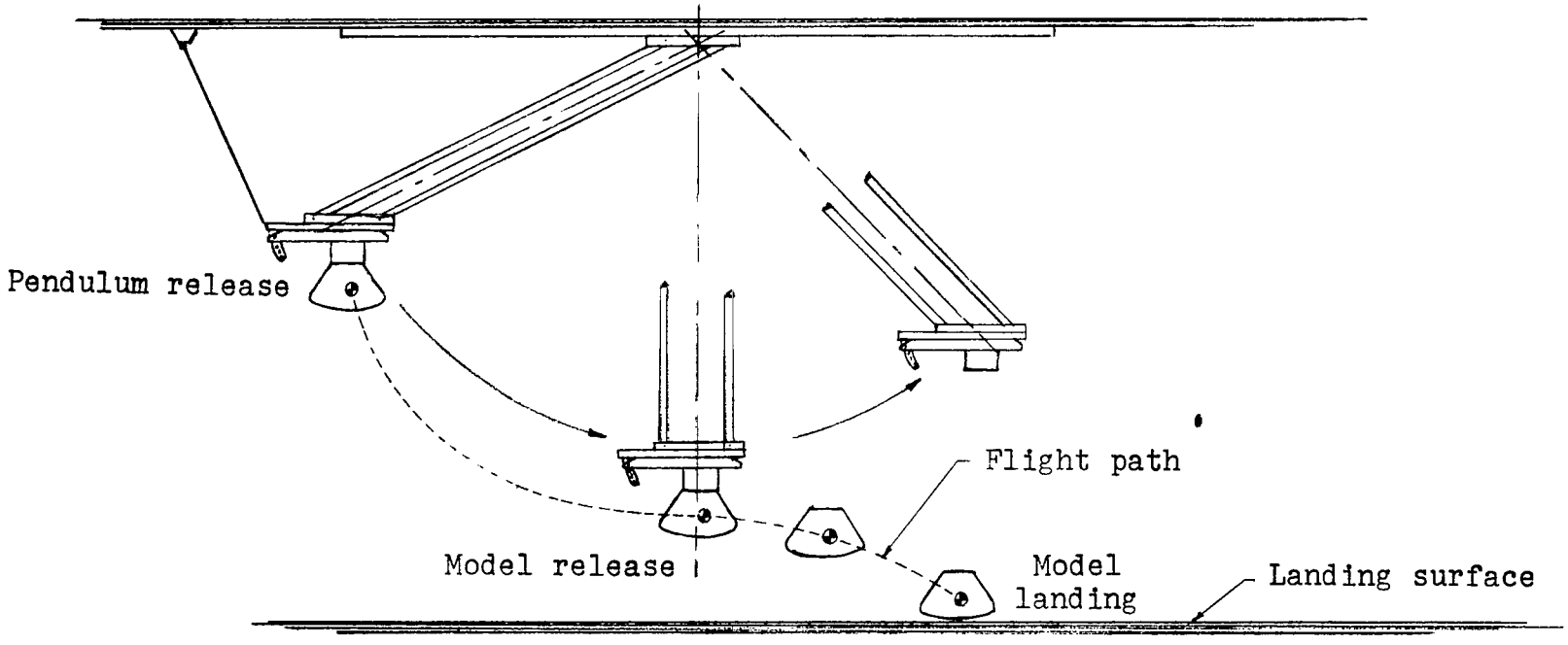

Figure 5.- Sketch showing pendulum operation during model launch and landing.

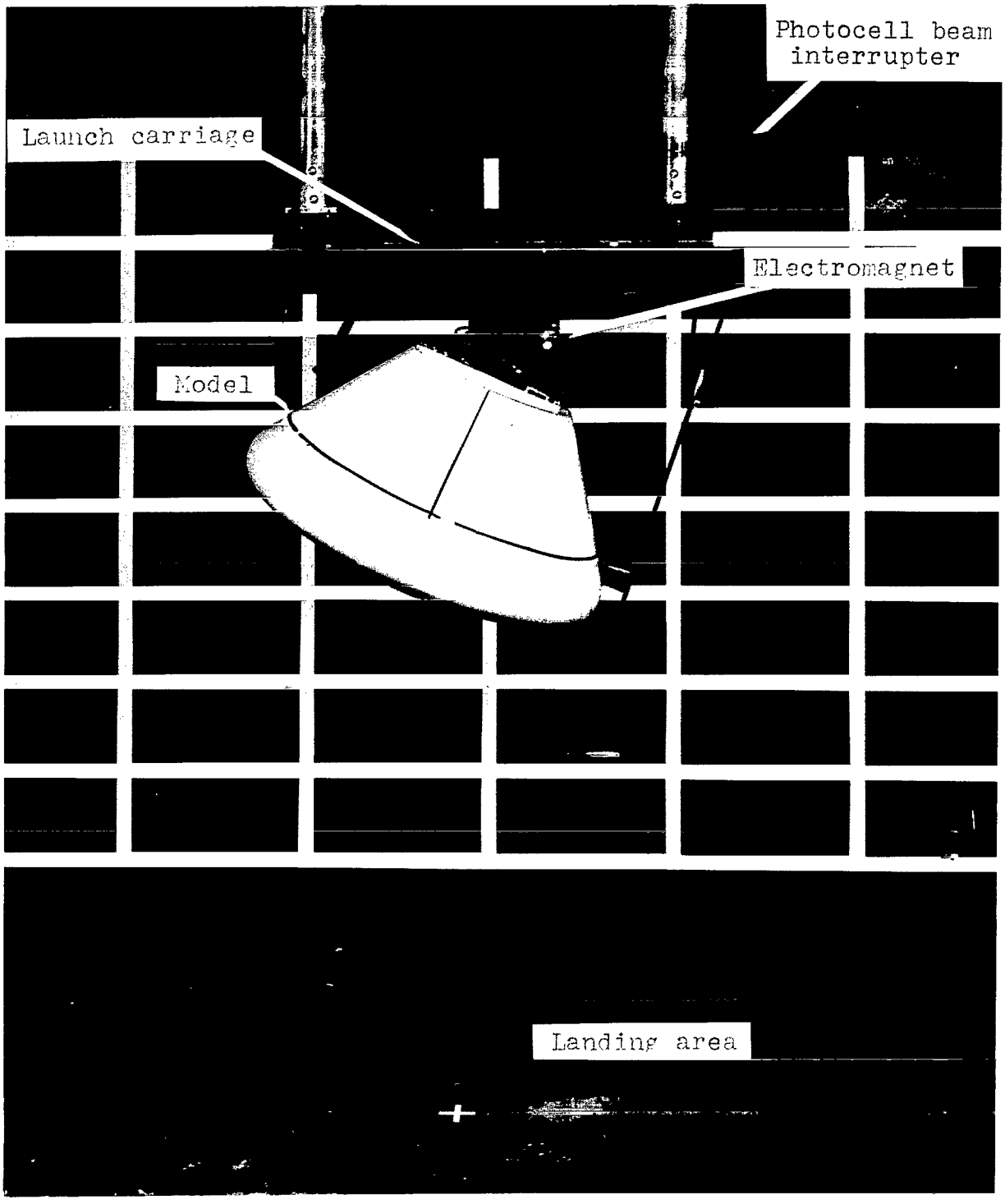

Figure 6.- Model on launch apparatus. L-62-4450.1

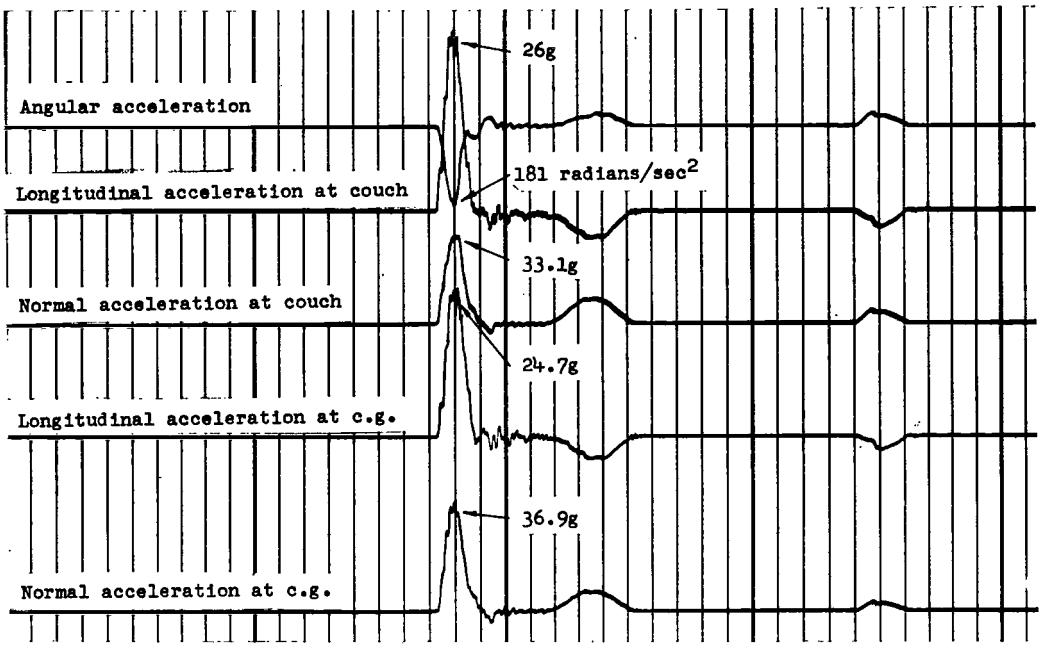

(a) Horizontal velocity, 0 ft/sec; landing attitude, -16°.

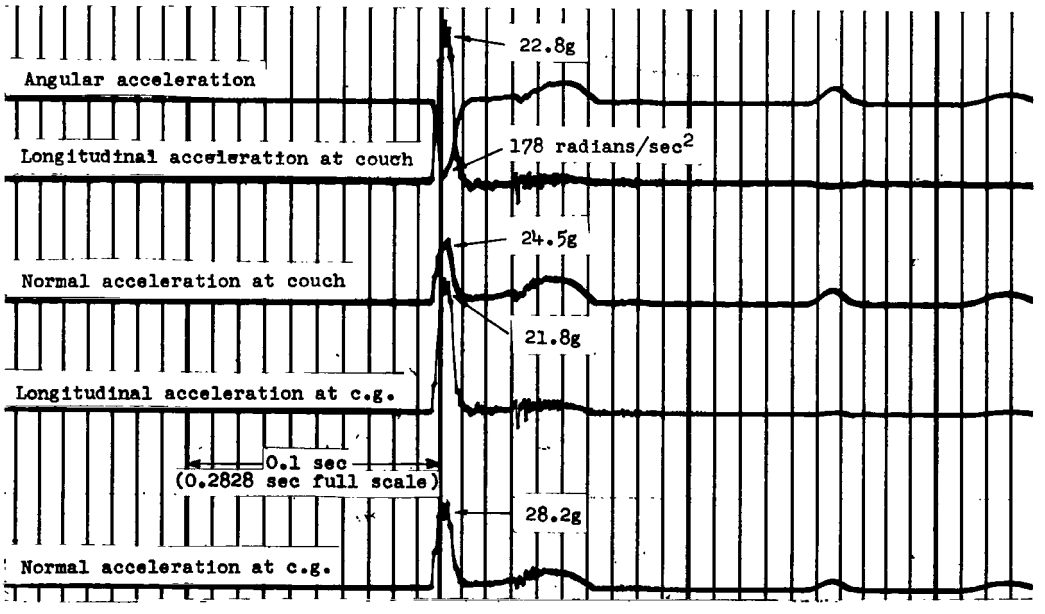

(b) Horizontal velocity, 30 ft/sec; landing attitude, -18°.

Figure 7.- Typical oscillograph records of accelerations for landings on a concrete surface. Vertical velocity, 30 ft/sec.

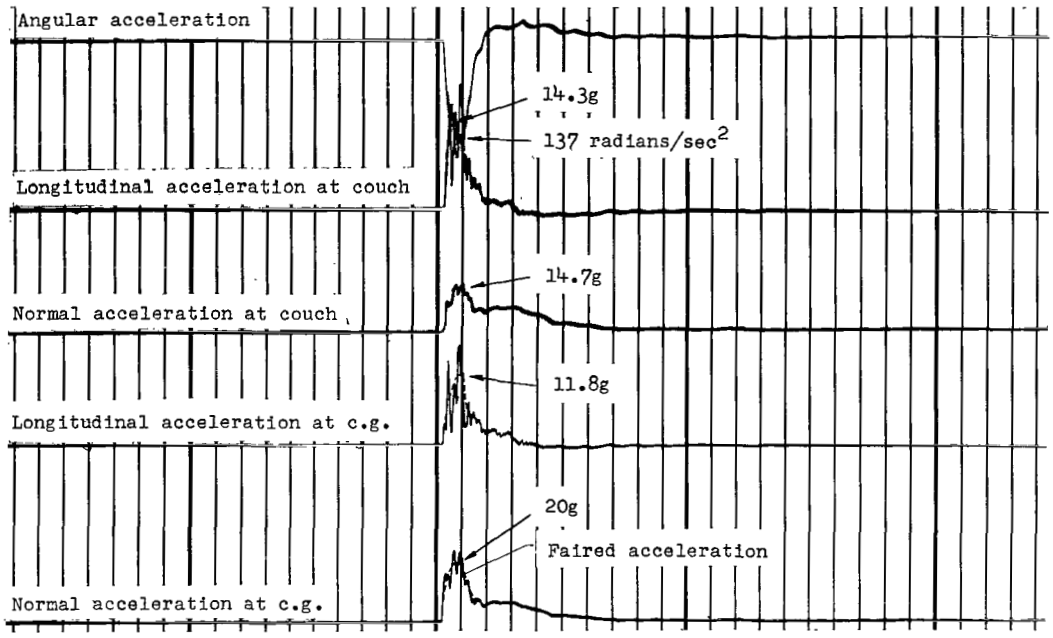

(a) Horizontal velocity, 0 ft/sec; landing attitude, -16°.

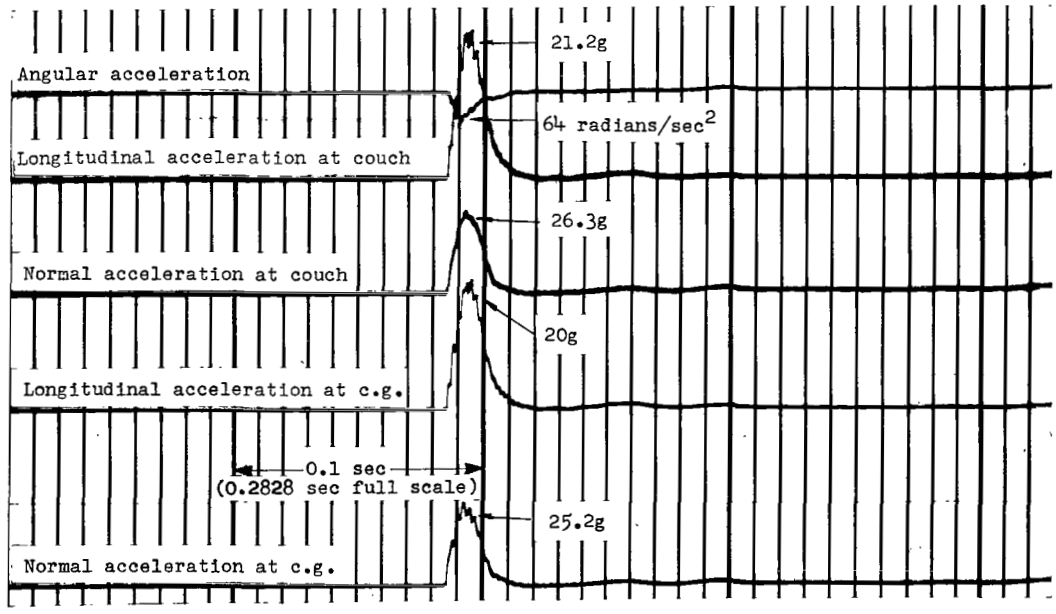

(b) Horizontal velocity, 50 ft/sec; landing attitude, -15°.

Figure 8.- Typical oscillograph records of accelerations for landings on sand. Vertical velocity, 30 ft/sec.

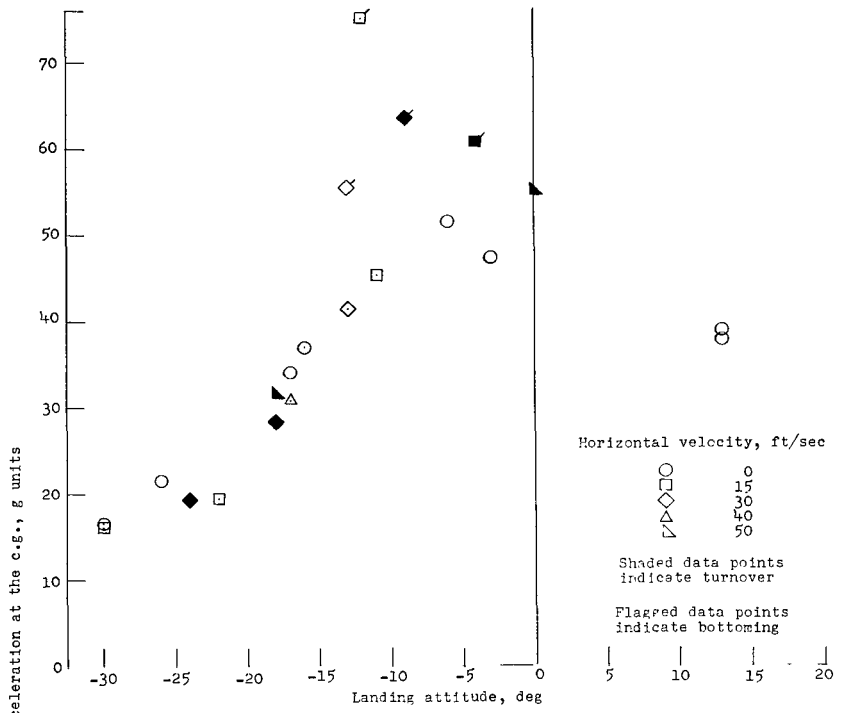

(a) Landings on a concrete surface.

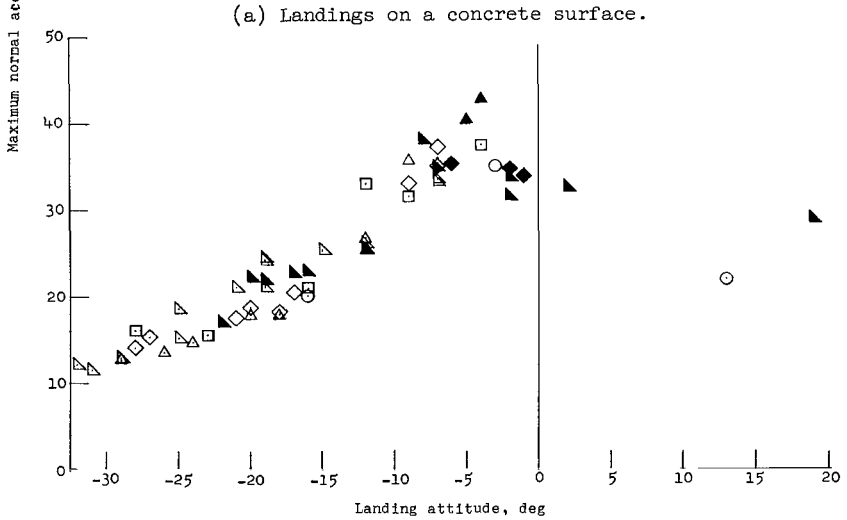

(b) Landings on sand.

Figure 9.- Maximum normal accelerations at the center of gravity of the vehicle. Vertical velocity, 30 ft/sec. (All values are full scale.)

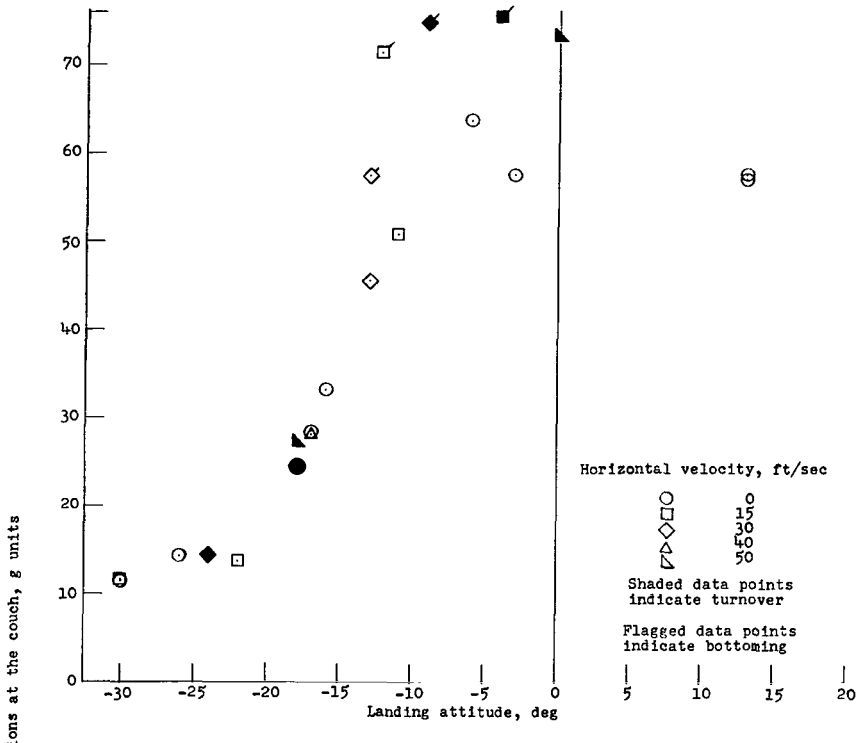

(a) Landings on a concrete surface.

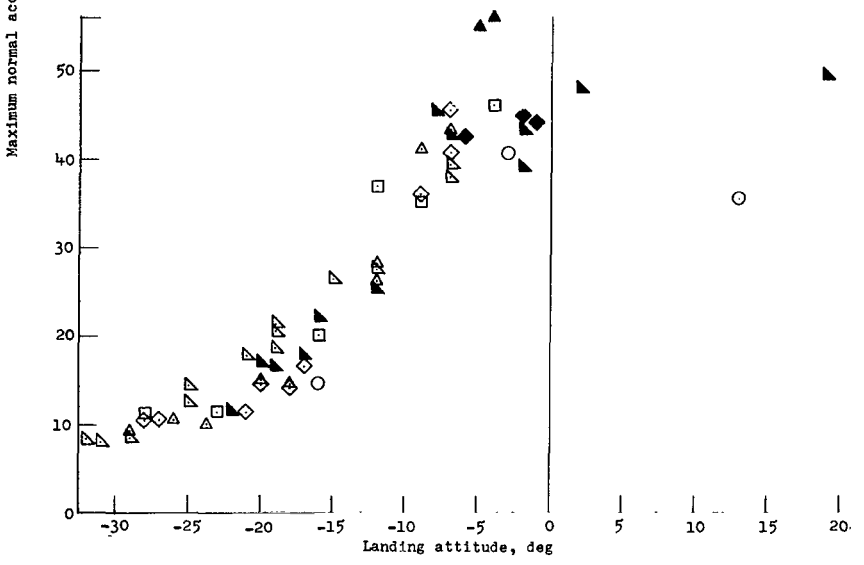

(b) Landings on sand.

Figure 10.- Maximum normal acceleration at the center of gravity of the couch. Vertical velocity, 30 ft/sec. (All values are full scale.)

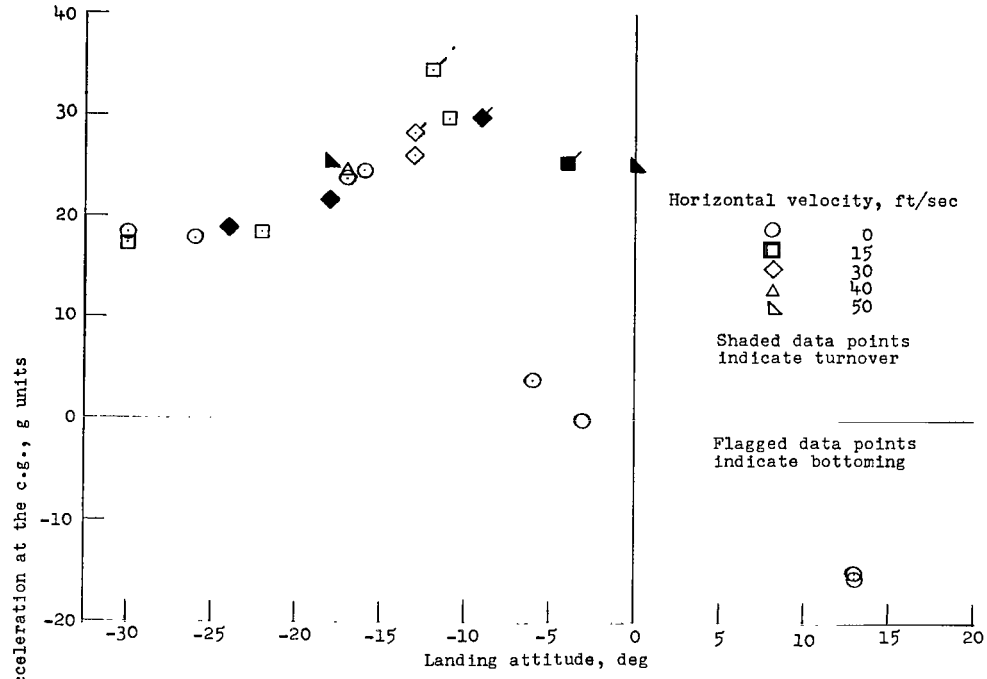

(a) Landings on a concrete surface.

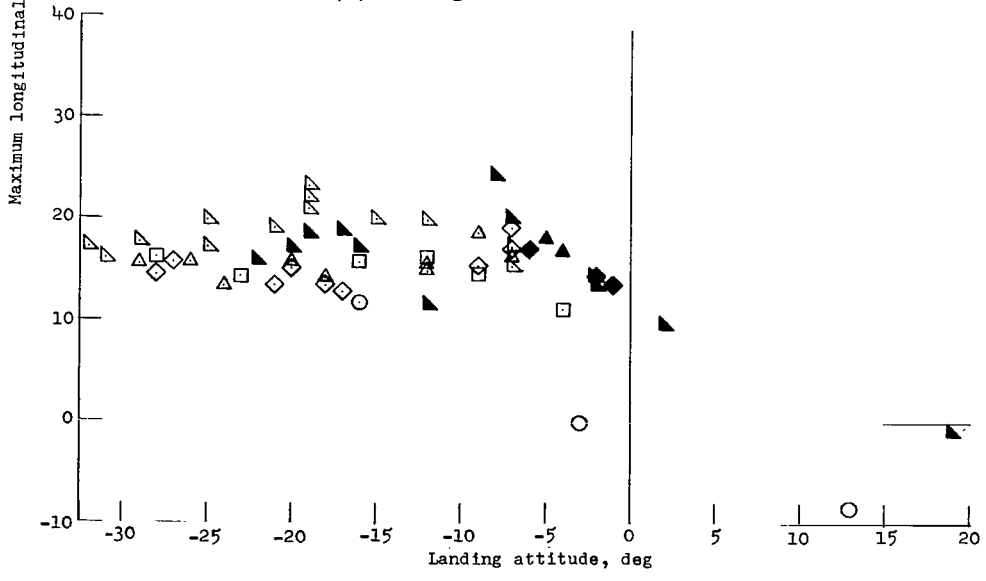

(b) Landings on sand.

Figure 11.- Maximum longitudinal acceleration at the center of gravity of the vehicle. Vertical velocity, 30 ft/sec. (All values are full scale.)

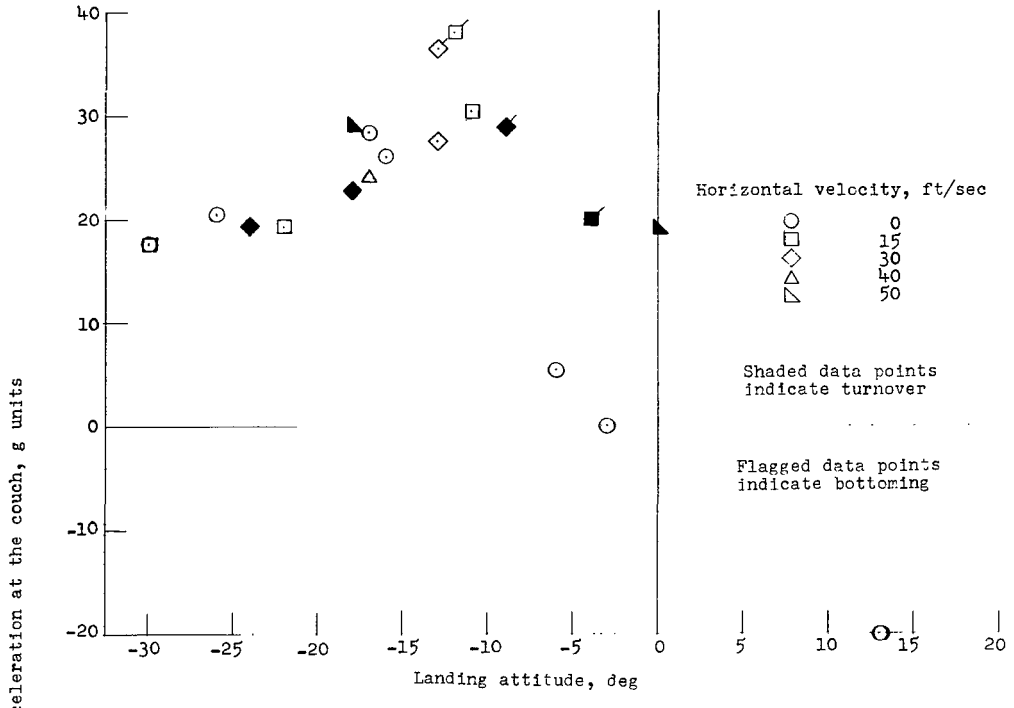

(a) Landings on a concrete surface.

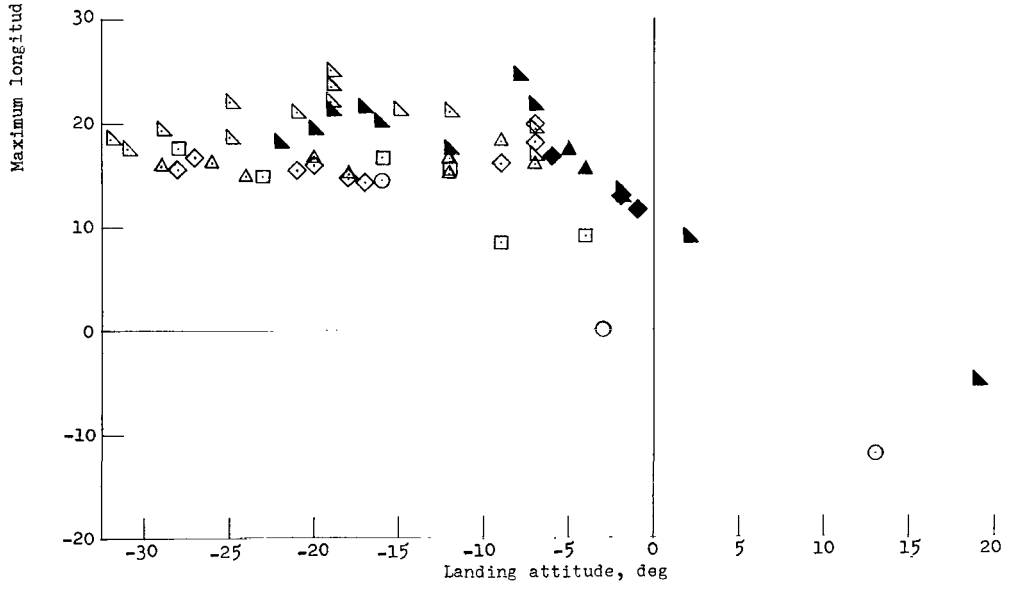

(b) Landings on sand.

Figure 12.- Maximum longitudinal acceleration at the center of gravity of the couch. Vertical velocity, 30 ft/sec. (All values are full scale.)

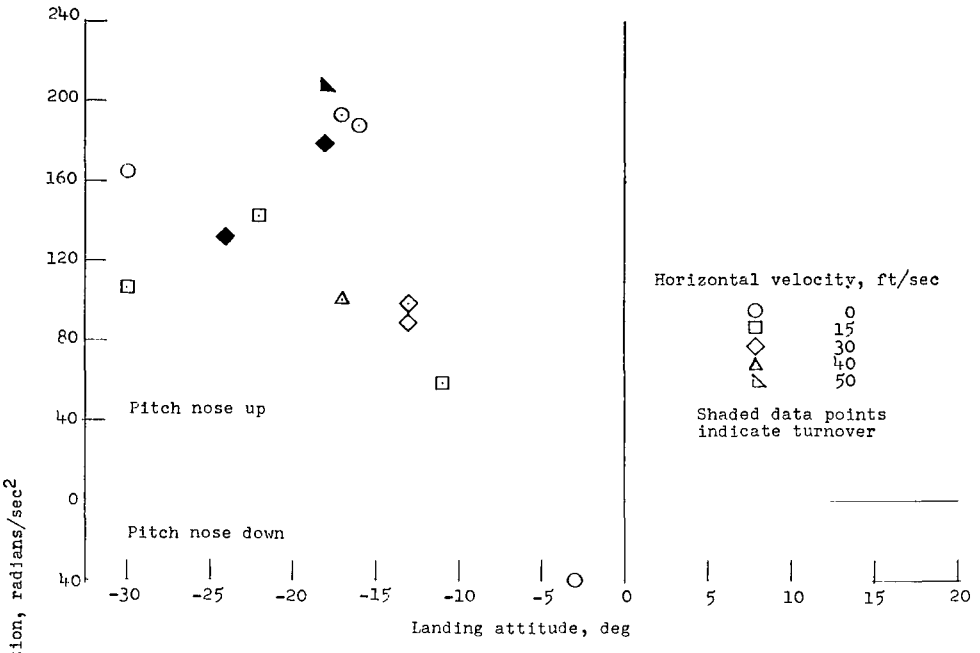

(a) Landings on a concrete surface.

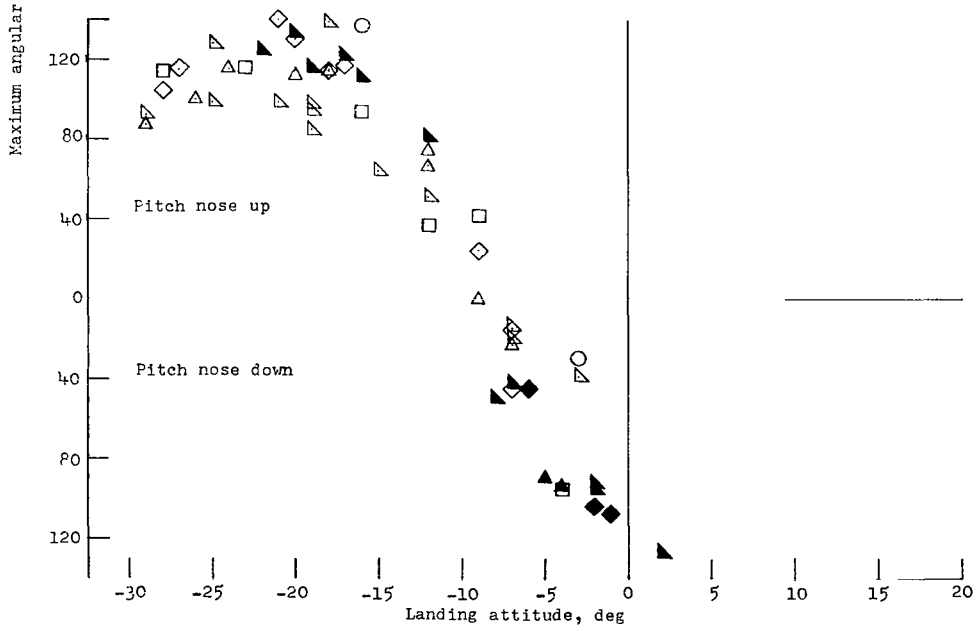

(b) Landings on sand.

Figure 13.- Maximum angular accelerations. Vertical velocity, 30 ft/sec. (All values are full scale.)

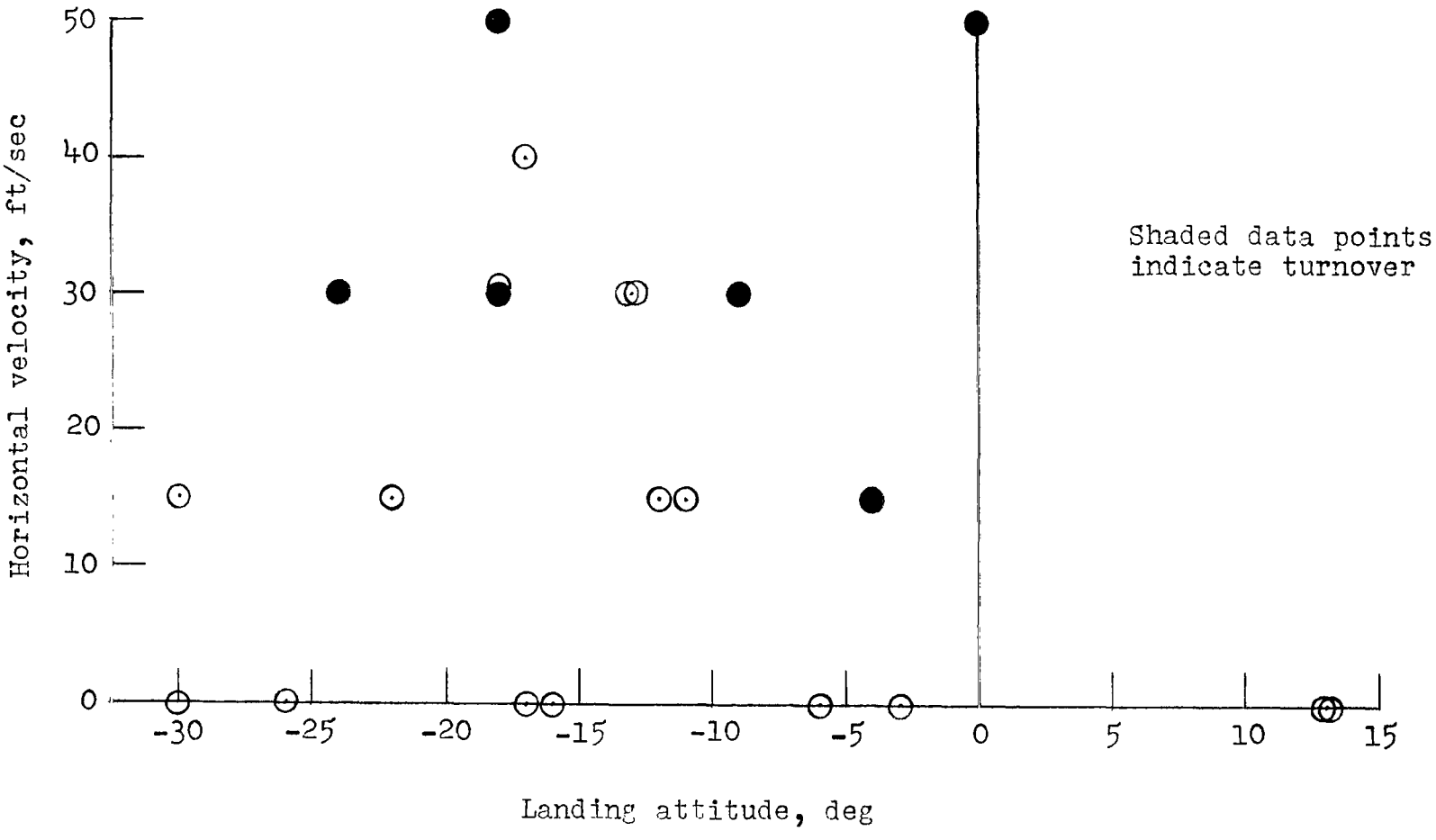

Figure 14.- Stability for landings on flat concrete. Vertical velocity, 30 ft/sec. (All values are full scale.)

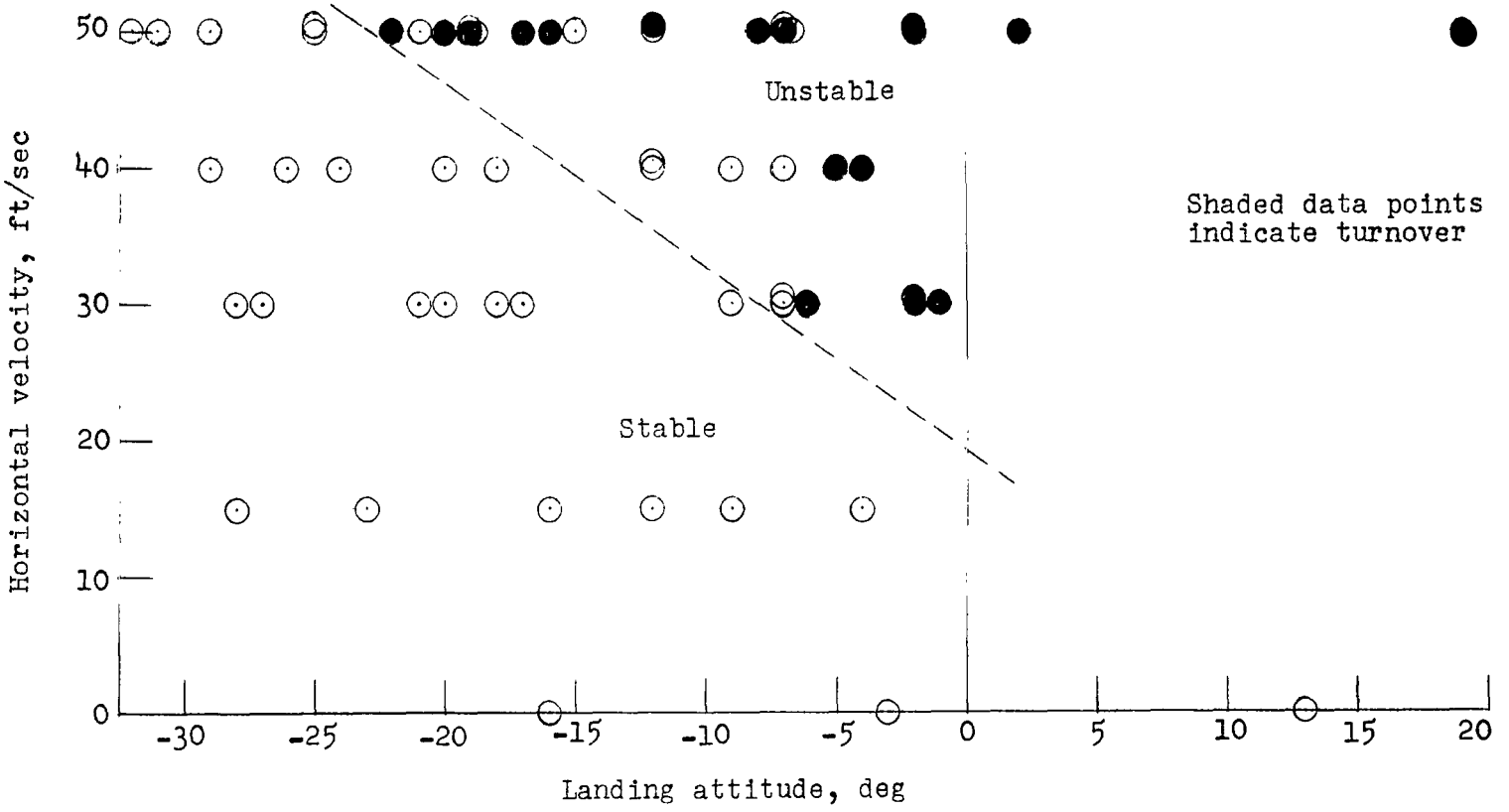

Figure 15.- Stability for landings on sand. Vertical velocity, 30 ft/sec. (All values are full scale.)